

PAPER



Cite this: *Soft Matter*, 2018, 14, 1434

A conductive hydrogel based on alginate and carbon nanotubes for probing microbial electroactivity†

Léopold Mottet,^a Domitille Le Cornec,^{id}^a Jean-Marc Noël,^b Frédéric Kanoufi,^{id}^b Brigitte Delord,^c Philippe Poulin,^c Jérôme Bibette^a and Nicolas Bremond^{id}^{*a}

Some bacteria can act as catalysts to oxidize (or reduce) organic or inorganic matter with the potential of generating electrical current. Despite their high value for sustainable energy, organic compound production and bioremediation, a tool to probe the natural biodiversity and to select most efficient microbes is still lacking. Compartmentalized cell culture is an ideal strategy for achieving such a goal but the appropriate compartment allowing cell growth and electron exchange must be tailored. Here, we develop a conductive composite hydrogel made of a double network of alginate and carbon nanotubes. Homogeneous mixing of carbon nanotubes within the polyelectrolyte is obtained by a surfactant assisted dispersion followed by a desorption step for triggering electrical conductivity. Dripping the mixture in a gelling bath through simple extrusion or a double one allows the formation of either plain hydrogel beads or liquid core hydrogel capsules. The process is shown to be compatible with the bacterial culture (*Geobacter sulfurreducens*). Bacteria can indeed colonize the outer wall of plain beads or the inner wall of the conductive capsules' shell that function as an anode from which electrons produced by the cells are collected.

Received 25th September 2017,
Accepted 16th January 2018

DOI: 10.1039/c7sm01929g

rsc.li/soft-matter-journal

Bacteria have been shown to be able to catalyse electrochemical reactions for either producing organic matter from CO₂¹ or to generate electricity from organic matter.² The development of microbial electrochemical technologies offers a perspective to capture a part of the energy contained in organic rich wastewater.^{3–5} Moreover, the use of such microbes for bioremediation of aquatic sediments and groundwater is also envisaged.^{6,7} In the most classical bioelectrochemical applications of microbial fuel cells, bacteria interact and exchange electrons at the surface of solid macroscopic electrodes.⁸ These electrodes are often made of a carbon material, because of its chemical inertness and biocompatibility. Biofilms develop at the surface of the electrodes (Fig. S1, ESI†). These substrates are convenient for implementation in electrochemical devices with adequate wiring and control. Nevertheless, they differ from natural substrates which are generally softer and permeable; they lose efficiency

because of the absence of permeability and fouling by thick biofilms. The use of porous scaffolds where carbon nanotubes are further coated⁹ or directly grown^{10,11} onto the macroporous substrate or even woven¹² has been shown to enhance the current densities of microbial bioelectrochemical systems. Confining bacteria in a biocompatible compartment would offer new opportunities to probe the electrochemical activity of bacteria in more favorable media. In addition, compartmentalizing bacteria in small compartments that are stacked inside an electrochemical cell could offer routes for the limitation of electrode fouling. Indeed, this strategy should facilitate the replacement of these compartments, containing dead microorganisms, by freshly encapsulated microbial colonies. Compartmentalization in permeable media would also allow more efficient nutrition and elimination of byproducts resulting from the electrochemical activity of the bacteria. Hydrogels can be shaped as compartments for entrapping cells,¹³ from solid to liquid cores.^{14,15} These materials act as a semi-permeable membrane and thus allow a rapid exchange of solutes with the surrounding.¹⁶ In that way, culture medium composition can be easily modified during cell growth. This compartment having a liquid core has been shown to be suitable for three-dimensional culture from microorganisms¹⁷ to mammalian cells.^{18,19}

From the microbial point of view, identifying the best adapted bacteria or consortium for a given physicochemical

^a Laboratoire Colloïdes et Matériaux Divisés, CNRS UMR 8231, Chemistry Biology & Innovation, ESPCI Paris, PSL Research University, 10 rue Vauquelin, 75005 Paris, France. E-mail: nicolas.bremond@espci.fr

^b Sorbonne Paris Cité, Paris Diderot University, Interfaces, Traitements, Organisation et Dynamique des Systèmes (ITODYS), CNRS-UMR 7086, 15 rue J. A. de Baïf, 75013 Paris, France

^c Centre de Recherche Paul Pascal – CNRS, University of Bordeaux, 115 Avenue Schweitzer, 33600 Pessac, France

† Electronic supplementary information (ESI) available. See DOI: 10.1039/c7sm01929g

environment and electrode features is of course of practical interest. For example, the apparition of a mutant of *Geobacter sulfurreducens* wild type strain generating a current density five times higher than the ancestral one has been isolated from a 5 months culture on an anode poised at 0.4 V.²⁰ Creating a technology that enables screening of various culture conditions, natural samples or inoculum is a promising way to discover new strains as previously demonstrated from the parallelization of 24 miniature microbial fuel cells (MFCs).²¹ An ideal evolution platform would be composed of parallelized compartments that have the ideal volume to allow an exponential amplification of any inherited characters acquired by cell communities, without expressing any bias initiated by physical or environmental heterogeneities. This would ensure a proper reading of the intrinsic microbiological detailed response leading to diversification, adaptation and evolution. However, considering electroactive bacteria, new bioreactors are needed in order to evaluate the electrochemical performances of cells, *i.e.* electron transfer from and to the cell colonies must be made possible.

Be it for selection of bacteria or other applications, the first critical challenge towards these novel conditions of microbial bioelectrochemical systems is the actual realization of permeable, biocompatible and conductive bioreactors. We aim at using electron conductive hydrogels for building a novel niche, having a core-shell structure, where the activity of exoelectrogenic bacteria can be assessed. Several strategies have been proposed for creating conductive hydrogels based on the mixture of polymers and conductive nanoparticles, like carbon based or metallic ones.^{22–24} Here, the process for making a composite hydrogel must satisfy several constraints: the rheological features of the dispersion should be suited to capsule formation, the whole process should be biocompatible and electron transfer between bacteria and the conductive network should be feasible. We propose to use a blend of alginate and carbon nanotubes initially dispersed with the help of surfactants. Alginate is chosen because of its biocompatibility and possible use to make permeable capsules of controlled size. Permeability is a critical feature to allow transport of nutriment and diffusion of byproducts of electrochemical reactions. Carbon nanotubes are chosen for two reasons. They are known to interact efficiently with electroactive bacteria because of their small dimensions.⁸ In addition, they can form percolated and therefore conductive networks at low volume fraction²⁵ so that the conductive gels remain soft and permeable.

In the following, the formulation of the colloidal mixture is first discussed. Then the conductive features of the composite hydrogel is probed by an electrochemical approach. Finally the selected conductive hydrogel formulation and process are challenged in the presence of exoelectrogenic bacteria, *Geobacter sulfurreducens*, one of the best candidates for microbial fuel cells.^{2,26}

1 Material and methods

Chemicals

Sodium alginate Protanal LF200FTS, provided by FMC Biopolymer, is composed of about 70% of guluronic acid and

has an average molecular weight of $1.5 \times 10^5 \text{ g mol}^{-1}$. Brij 35, Brij 58, Brij 78, sodium dodecyl sulfate (SDS), sodium oleate, Tween 20, poly(ethylene) glycol ($M_w = 3.2 \times 10^3 \text{ g mol}^{-1}$), barium chloride, potassium chloride and ferrocenemethanol (FcMeOH) were all purchased from Sigma Aldrich and used without any further purification. Carbon nanotubes (CNTs) labelled Graphistrength C100 (Arkema) are multiwalled nanotubes with a diameter of about 10–15 nm. All solutions were made by using ultra pure water (Milli-Q).

Solution preparation and characterization

Carbon nanotubes are dispersed in water at a concentration of 2 wt% by sonication in the presence of surfactants. The dispersion is performed by using a sonicator (VibraCell 750W) equipped with a 3 mm diameter probe. The dispersion is realized with a volume of 10 mL at 35% of the maximal power with alternating pulses of 3 s separated by 1 s for 1 h and 15 min. The solution is maintained in a bath of ice in order to avoid overheat. The fine particle dispersion of carbon nanotubes is verified under an optical microscope. The alginate powder is then added to the CNT dispersion which is finally mixed for 12 h under magnetic stirring to obtain the final alginate/CNTs/surfactant solutions at desired CNT concentrations (Fig. 1). The final concentration of alginate is set to 1 wt%.

The rheological properties of the solutions are characterized using a rheometer (AR1000, TA Instruments) in a Couette geometry. The surface tension of the solutions is determined using the pending drop method (DSA30, Krüss). For the CNT dispersions, the samples are first centrifuged at $8000 \times g$ for 1 h and the surface tension of the supernatant is then evaluated.

Composite bead formation

The alginate/CNTs mixture is dripped into a barium chloride bath at a concentration of 1 wt% from a 2 mm diameter needle at a height of 5 cm (Fig. 1). Barium ions induced a quick gelation of the alginate at the periphery of the drops which are then kept in the bath for 2 h under slight agitation to ensure complete gelation *via* the diffusion of barium ions towards the beads' center. The resulting beads' diameter is 3.5 mm as measured from image analysis. Hydrogel beads are then added to a large amount of pure water and kept immersed for 48 h. As discussed in Section 2.2, this step allows to wash away surfactants from CNTs, like a dialysis where the alginate hydrogel plays the role of a semi-permeable membrane. After this dialysis step, beads are stored in a BaCl₂ solution (1 mM). They are ready to be used for further experiments (electrochemistry/current production with bacteria). We note that barium ions are used instead of calcium, which are commonly used to crosslink alginates, since we noticed the formation of a precipitate in the culture medium in the presence of calcium but not with barium.

Geobacter sulfurreducens strain and culture

The *Geobacter sulfurreducens* strain used during this study is a PCA strain provided by DMSZ (DMS12127). Its nutrient medium has been realized in the lab according to the DMSZ protocol for *Geobacter* medium 826 completed by 0.1 mM of BaCl₂.

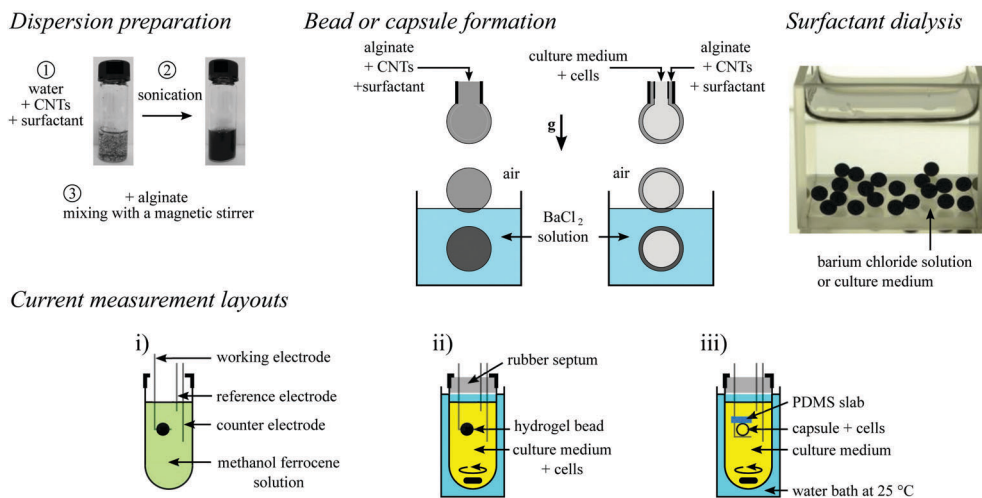


Fig. 1 Protocol to form beads or liquid core capsules made of alginate and CNTs along with the layouts of electrochemical characterization of (i) the composite hydrogel, the current generated by a biofilm that develops (ii) onto a bead or (iii) inside a liquid core capsule.

Here, the soluble electron acceptor is fumarate. Cultures are initiated by dilution by 10 of the stock culture in the growth medium in a hungate tube sealed with a butyl-rubber plug non-permeable to gas. Before incubation, the culture is kept under anaerobic conditions by bubbling a gas mixture (80% N_2 , 20% CO_2) for 20 min. The culture is then incubated at 30 °C under orbital agitation. The growth is followed by absorbance measurement at 600 nm using a UV-spectrophotometer.

G. *sulfurreducens* encapsulation

The process for creating liquid core capsules is based on a co-extrusion method.¹⁷ In such a method, a double drop having an outer part made of alginate/CNTs solution and a core composed of culture medium and cells can be created (Fig. 1). The shell solidifies once the compound drop falls into a $BaCl_2$ bath. Like beads, capsules have an average size of 3.5 mm. Traces of surfactants, Tween20, are added to the gelling bath and 1 mM of SDS is supplemented to the shell solution to ensure proper engulfing of the compound drops and thus successful capsule formation.¹⁷ The core solution is composed of a culture in a stationary state, which is further diluted 10-fold in a polyethylene glycol solution at 10 wt% for increasing the core viscosity and thus ensuring sphericity of the capsules. The ratio between the core and the shell flow rates, which sets the shell thickness, is equal to 2.5 when the cell growth is measured and to 1.25 when the current of encapsulated bacteria is probed. The double drop is dripped from a concentric double needle where the external one has a diameter of 3 mm at a height of 5 cm into a barium bath at 1 wt%. The capsules are transferred to a fresh culture medium after having spent 5 min in the gelling bath. For the cell growth inside capsules, the culture medium is replaced 2 h after the beginning of the culture, after 24 h and then kept in *G. sulfurreducens* culture conditions for 1 week. For monitoring the growth of encapsulated bacteria by absorbance measurements, a capsule is first burst in a tube containing culture medium and then strongly agitated for 1 min with the help of a vortex mixer.

Electrochemical characterization

Cyclic voltammograms and current measurements are obtained using a 3 electrode system controlled by a potentiostat (CH Instruments, 62A03). The electrode system is composed of an $Ag(s)/AgCl(s)$ reference electrode, a platinum grid as the counter-electrode and a platinum wire (250 μm in diameter) as the working electrode (WE). For beads, the platinum wire pierces the bead from side to side (Fig. 1(i) and (ii); Fig. S2(i) and (ii), ESI[†]). For capsules, the connexion is made by gently pressing the platinum wire to the capsule shell with the help of a reticulated poly-dimethylsiloxane (PDMS) slab that has been previously pierced by the working electrode (Fig. 1(iii) and Fig. S2(iii), ESI[†]).

2 Results and discussion

2.1 Formulation

Carbon nanotubes are natively hydrophobic, and therefore a stable dispersion of CNTs in water requires either chemically modifying their surface²⁷ or using polymers²⁸ or surfactants.²⁹ As discussed later on, only the surfactant based strategy allows ending up with a conductive network of CNTs. The addition of charged surfactants like SDS is known to lead to well dispersed CNTs thanks to electrical repulsion between solid particles.³⁰ Unfortunately, the homogeneity of the CNT dispersion is altered when alginate is added as revealed by the optical micrographs reported in Fig. 2(a). Large aggregates of CNTs of a few tens of micrometers are present in the dispersion. This impacts the fluidity of the mixture. Indeed, while exhibiting shear thinning behavior, the viscosity at zero shear rate increases by almost two orders of magnitude as compared to a pure alginate solution (Fig. 2(a)). In previous work,³¹ we were able to form plain beads with SDS and to characterize their properties by various electrochemical techniques, including local electrochemical mapping which also revealed the heterogeneity of the CNT dispersion. However, the rheological features of the colloidal mixture when

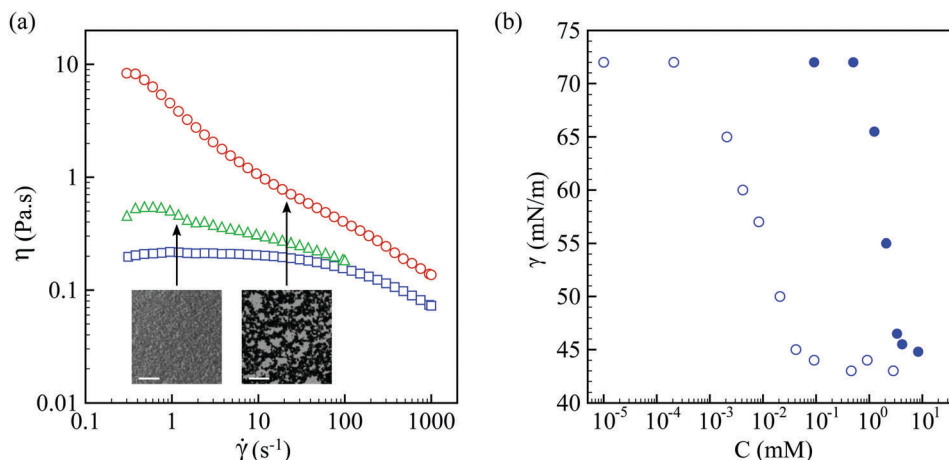


Fig. 2 (a) Flow properties of the blend of alginate (1 wt%) and CNTs (1 wt%) dispersed with SDS (○) and Brij (△) along with the corresponding microscope images of the mixtures (scale bar is 100 μm). For comparison, the viscosity of a solution with the same amount of alginate but without CNTs is also shown (□). (b) Surface tension of water as a function of Brij35 concentration with 1 wt% of CNTs (●) and without (○).

SDS is used do not allow to properly form liquid core capsules. The use of another anionic surfactant having a longer carbon chain, sodium oleate, and thus a higher energy of adsorption does not prevent such flocculation. On the other hand, when a non-ionic surfactant, Brij35, having the same hydrophobic chain as that of SDS is used, the dispersion is homogenous while the viscosity slightly increases (Fig. 2(a)). The destabilization mechanism is possibly different from a bridging scenario where polymers displace surfactants from the CNT surface.³² Here, the flocculation might be due to the nature of alginate which is a negatively charged polyelectrolyte carrying thus a cationic counter ion, *e.g.* like a sodium ion for SDS. The presence of sodium ions indeed reduces electrostatic repulsion and thus favors aggregation.

Non-ionic surfactants are therefore selected to disperse CNTs. The required amount of surfactant molecules for good dispersion of CNTs in water is determined by measuring the surface tension of the dispersions. The evolution of the surface tension as a function of surfactant concentration, here Brij35, with and without CNTs is reported in Fig. 2(b). In the absence of CNTs, the critical micellar concentration (CMC) of Brij35 is found at 0.1 mM. Once 1 wt% of CNTs is added to the surfactant solution, the CMC is shifted to about 4 mM. This CMC displacement is a signature of the adsorption of surfactant molecules onto the CNT surface. For the experiments reported in the following, a concentration above the CMC is used, and it is typically chosen to equal 6.5 mM.

2.2 A conductive hydrogel

After homogenization of the alginate/CNTs mixture, and thanks to its shear thinning behavior, composite hydrogel beads or capsules can be easily processed by extrusion (Fig. 1). The flow rates of the solutions are set such that drops are formed in a dripping regime. The drops are collected in a barium chloride solution that turns the mixture into a gel. Using a surfactant allows prevention of aggregation of hydrophobic particles, which is needed for obtaining a homogenous mixture with alginate, but thus also prevents electrical conduction between

CNTs. Surfactant molecules must then be washed away to connect CNTs. Composite hydrogel beads are thus left in a large reservoir of water free of surfactants in order to induce surfactant desorption.

The electrical properties of composite hydrogel beads are assessed using electroanalytical methods. Beads are first immersed into a barium chloride solution (1 mM) having a volume 1000 times larger than those of beads. Then, at a given time, a bead is plunged into a ferrocenemethanol solution (1 mM) for 30 minutes in order to saturate the bead in FcMeOH due to its ability to permeate the composite hydrogel.³¹ The bead is finally pierced using a thin platinum wire which is connected to a potentiostat, and plunged in a cell containing FcMeOH solution (1 mM) along with the counter electrode and the reference electrode (Ag/AgCl) as sketched in Fig. 1(i). The medium is completed with KCl (0.1 mM) and BaCl₂ (1 mM). A cyclic voltammogram (CV) is then performed at a scan rate of 10 mV s⁻¹. Examples of such CVs are given in Fig. S1 (ESI[†]), while that of a percolated bead is reported in the inset of Fig. 3(a). An oxidation feature is observed on the CVs, corresponding to the oxidation of FcMeOH at the conductive assembly. From such a measurement, an oxidation peak current denoted as i_p can be estimated. The impact of the dialysis time on i_p is shown in Fig. 3(a) for three different surfactants. These surfactants, Brij35, Brij58 and Brij78, possess a hydrophobic tail made of 12, 16 and 18 atoms of carbon, respectively. All experiments were performed with an initial amount of surfactants in excess. For the longer chain Brij78, the measured peak current is constant during the time period of the experiment that lasts almost for 7 days. The signal is simply due to the oxidation of FcMeOH at the platinum wire's surface, suggesting that the bead is not conductive (no percolation of the CNT network). For a slightly smaller chain Brij58, the current starts to increase after 3 days of dialysis. On the other hand, for Brij35, the current slowly increases during the first 14 h where its value is multiplied by 3. Then, i_p undergoes a thirtyfold increase during the next 10 h, *i.e.* after 1 day. The oxidation peak current finally slowly increases; its

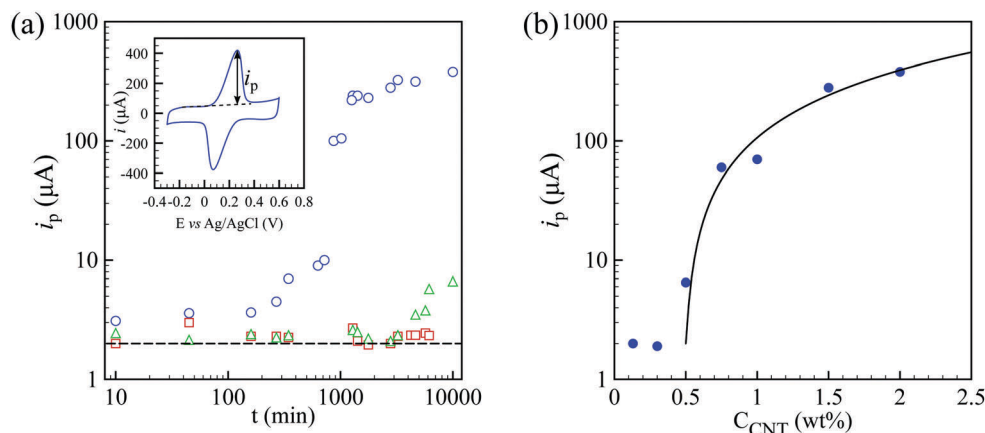


Fig. 3 Electrochemical characterization of composite hydrogel beads dispersed in ferrocenemethanol solution (1 mM) in a layout shown in Fig. 1(i). (a) Time evolution of the oxidation peak current i_p during the dialysis of beads made from CNTs (1.5 wt%) dispersed with different surfactants: Brij78 (\square), Brij58 (\triangle) and Brij35 (\circ). The dashed line corresponds to the response of the platinum electrode alone. Inset: Cyclic voltammogram recorded at a scan rate of 10 mV s^{-1} for a percolated bead. (b) Variation of the oxidation peak current as a function of the CNT content after complete dialysis of surfactant molecules (Brij35). The continuous line represents a critical-like function that describes the percolation of the CNT network, i.e. $i_p = i_p^0 + i_p^m(C_{\text{CNT}} - C_{\text{CNT}}^c)^\beta$ where $i_p^0 = 2 \mu\text{A}$, $i_p^m = 240 \mu\text{A}$, $C_{\text{CNT}}^c = 0.5 \text{ wt\%}$ and $\beta = 1.2$.

value is only multiplied by 1.5 for the 6 following days. This slow dynamics where stress relaxation induces network reorganization has been observed for physical hydrogels like the alginate one.³³ The CV shape changes to a bell-shaped feature (inset of Fig. 3a) while the peak current increases (the time evolution of CV shapes is reported in Fig. S3, ESI[†]). The bell-shape suggests the complete consumption of ferrocenemethanol within the composite hydrogel bead. By choosing the right surfactant, which is non-ionic and has a low adhesion energy towards CNTs, it is possible to homogeneously mix CNTs with alginate and to induce effective electrical contacts between the particles after dialysis. The composite hydrogel finally works like a porous electrode. The first matrix is made of alginate that is ionically cross-linked and ensures mechanical stability to the hydrogel and a second network made of carbon nanotubes, probably in contact *via* van der Waals forces,³⁴ provides electronic conductivity.

We wonder now how the conductivity features of the composite hydrogel depend on the amount of CNTs. Hydrogel beads containing various mass fractions of CNTs with 1 wt% alginate were then produced. After a dialysis period of about 1 week, the beads were assessed using electroanalytical methods as previously discussed. The evolution of the oxidation peak current of ferrocenemethanol *versus* the concentration of CNTs, C_{CNT} , exhibits a classical percolation behavior (Fig. 3(b)). The conductivity is null for low amounts of particles and then sharply increases above a critical concentration C_{CNT}^c . The evolution of the oxidation peak current, linked to a modification of the network connectivity, is described by a critical-like function, i.e. $i_p = i_p^0 + i_p^m(C_{\text{CNT}} - C_{\text{CNT}}^c)^\beta$, where i_p^0 is the peak current for FcMeOH oxidation at the the platinum wire alone. The corresponding critical concentration is equal to 0.5 wt% and $\beta = 1.2$. This low percolation threshold is due to the anisotropic shape of the CNTs²⁵ but it is larger than that for single wall CNTs³⁵ while being close to the reported values for bundles of CNTs.³⁶

2.3 Probing bioelectroactivity of bacteria with a composite hydrogel

Before using such a composite hydrogel as an electrode for probing bio-electroactivity, the bio-compatibility of the process is first assessed. The growth of bacteria is evaluated from turbidity measurements. The difference of absorbance between the cell suspension and the culture medium measured at 600 nm, ΔOD_{600} , as a function of time is reported in Fig. 4. The value of ΔOD_{600} at $t = 0$ is extrapolated from the optical density of the initial cell suspension and further diluted before encapsulation. The cell number is assumed to be proportional to ΔOD_{600} . As expected for cell culture in bulk, the cell number first increases exponentially and then saturates at $\Delta\text{OD}_{600} \sim 0.7$, probably when all acetate has been consumed, as previously

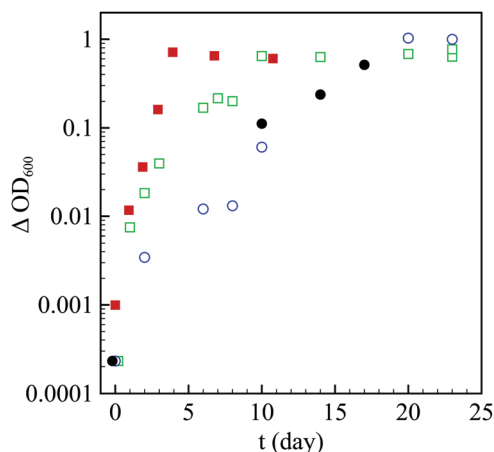


Fig. 4 Growth of *G. sulfureduccens* in bulk at $T = 30 \text{ }^\circ\text{C}$ (\blacksquare), in a liquid core capsule having either an alginate hydrogel membrane at $T = 30 \text{ }^\circ\text{C}$ (\square) and at $T = 25 \text{ }^\circ\text{C}$ (\circ) or a composite shell at $T = 25 \text{ }^\circ\text{C}$ (\bullet). ΔOD_{600} represents the difference of absorbance between the cell suspension and the culture medium measured at 600 nm.

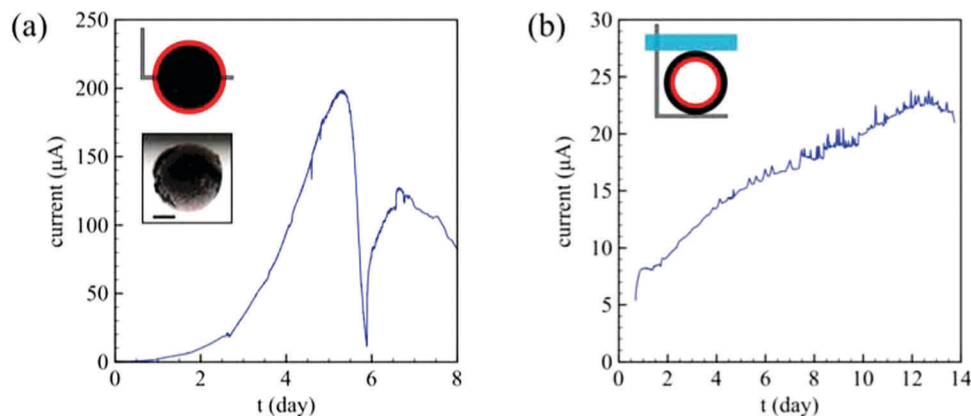


Fig. 5 (a) Chronoamperometry of a biofilm of *G. sulfureducens* growing on a composite hydrogel bead. The fall of the current followed by a rising signal corresponds to a renewal of the culture medium. The schematics illustrates how the bead is connected to the potentiostat. The image is a snapshot of the bead after 7 days of incubation (scale bar is 1 mm). (b) Chronoamperometry of a biofilm developing inside a liquid core capsule having a composite hydrogel membrane. The schematics illustrates how the capsule is compressed by a PDMS slab (in blue) onto the platinum wire connected to the potentiostat. For both schematics, the red layer represents the biofilm. The anode is poised at 0.4 V (versus Ag/AgCl electrode) for both conditions.

reported.³⁷ In the exponential, phase, the corresponding division time is about 10 hours. For bacteria encapsulated in capsules having a hydrogel shell without CNTs, the growth rate is initially similar to the bulk one, then slows down and finally the cell concentration saturates at the same level. We stress that the optical density difference, and thus the cell concentration, for encapsulated cells is evaluated by taking into account the surrounding culture medium. Therefore, the cell concentration inside the capsule is much higher than the corresponding culture in bulk. The cell number is indeed multiplied by the volume ratio between the external medium and the capsule's one. Cells are thus able to grow in a crowded environment without impeding their growth rate. Starting from the stationary phase, the cell number can even double if the surrounding culture medium is replaced. When adding CNTs to alginate, which requires the use of surfactants and a dialysis step, the bacterial concentration reaches the same level. We note that the growth rate is similar to a culture in capsules at the same temperature but without CNTs. To conclude, the whole process of encapsulation within composite hydrogel capsules is thus compatible with cell culture.

The next step is then to verify whether or not cells are able to attach to the composite hydrogel when fumarate, a soluble electron acceptor, is depleted. Plain beads are first prepared and then hooked by a platinum wire. The wired hydrogel bead is immersed in a culture medium with cells at a concentration close to that of the saturation phase, but free from fumarate. The system is finally maintained at 25 °C under stirring and anaerobic conditions (Fig. 1(ii)). Time evolution of the current when a wired bead made of 2 wt% CNTs is poised at 0.4 V (versus Ag/AgCl electrode) is reported in Fig. 5(a). Poising the anode at a slightly positive potential allows avoiding electron transfer limitations.^{38,39} The current increases up to about 200 µA at day 5 and then sharply decreases. Then the current increases again once the culture medium is replaced at day 6. As seen from the snapshot reported in Fig. 5, a biofilm developed around the composite bead. Pieces of the biofilm have been detached during manipulation, mainly while replacing the

culture medium that required to bubble the gas mixture free from dioxygen, explaining why a lower maximum current is then obtained. With the bead's diameter being 3.5 mm, the corresponding maximal current density, for a fully covered surface, is about 5 A m⁻². This value is comparable with those of previous experiments using anodes made of a carbon based material.^{31,40} A biofilm developed on a composite bead containing 1.5 wt% CNTs exhibits a maximal current density of around 4 A m⁻², a smaller value than the previous hydrogel composition but consistent with lower electrical conductance (Fig. 3(b)).

The current delivered by encapsulated bacteria in a liquid core composite hydrogel capsule is finally assessed. Here, the capsule shell contains 1.5 wt% CNTs and have a diameter of 3.5 mm. Piercing the capsule using a platinum wire is not possible because of a weaker mechanical resistance. The capsule is thus sandwiched between a platinum wire and a slab of PDMS (Fig. 5(b) and Fig. S2(iii), ESI†). When bacteria are encapsulated, the current is observed to increase with time and reaches a maximal value of about 22 µA. By assuming a perfect spherical geometry and by mass conservation during the co-extrusion of the core and the shell solutions, the inner capsule surface is 0.67 smaller than the outer one. The maximal current density is then around 0.9 A m⁻². This value is smaller than a plain bead which might be attributed to a higher electrical resistance between the capsule's shell and the platinum wire. Indeed, as observed for beads, such a connexion leads to a higher electrical resistance since the anodic peak current (i_p) in a ferrocene methanol solution is about 2.5 times lower than that for a pierced bead (data not shown). However, the use of such a conductive hydrogel capsule as an anode is demonstrated to be compatible with the encapsulation of electroactive bacteria that are then able to survive under anaerobic conditions.

3 Conclusion and perspectives

Here, we propose a novel materials science based strategy to open opportunities in the field of electrobiocatalysis upon

application to microbial fuel cells. Our approach lies in the design of hollow spheres made of a semi-permeable conductive shell used to encapsulate growing electrochemically active bacteria colonies. Carbon nanotubes and alginate are homogeneously mixed by surfactant assisted dispersion followed by a desorption step that triggers electrical conductivity. The type of optimal surfactant and the amount of CNTs have been determined for being compatible with a liquid core capsule formation process based on a co-extrusion step in air followed by a gelling step in an aqueous solution. The whole process is shown to be biocompatible. The compartmentalization of the biofilm formation allows isolation of individuals and thus would help in revealing the diversity among or between species. The ability to select a specific colony, generating the highest current for example, that will then be used to inoculate a new set of capsules opens the way to directed evolution experiments. A next step would be then to design a screening platform where the fate of many colonies entrapped in such bioreactors could be possible. Our approach should lead to broader applications in the field of electrobiocatalysis. Cooperation between strains among biofilms has been demonstrated to be a key feature for MFC in natural environments. Such compartmentalized cell culture offers unique capability to further investigate the interplay between specific strains by co-encapsulation. Also, the screening platform could be used to identify efficient bacteria or consortium from natural samples. The present study focused on the growth of microbial colonies at an anode for extracting electrons, but such a strategy could also be used to probe the metabolism of bacteria that accept electrons from a cathode.^{41,42} The selected bacteria strains could then be used at both working electrodes of a MFC.⁴³ Moreover, this would have an impact on applications relying on the conversion of CO₂ to organic matter using biocatalysis and solar energy.^{1,44}

Conflicts of interest

There are no conflicts to declare.

Acknowledgements

We thank the SIMM group from ESPCI Paris for giving us access to their rheometer. LM is funded by CNRS in the framework of "Mission pour l'Interdisciplinarité".

References

- 1 K. P. Nevin, T. L. Woodard, A. E. Franks, Z. M. Summers and D. R. Lovley, *mBio*, 2010, **1**, e00103–e00110.
- 2 B. E. Logan, *Nat. Rev. Microbiol.*, 2009, **7**, 375–381.
- 3 M. T. Agler, B. A. Wrenn, S. H. Zinder and L. T. Angenent, *Trends Biotechnol.*, 2011, **29**, 70–78.
- 4 B. E. Logan and K. Rabaey, *Science*, 2012, **337**, 686–690.
- 5 P. Pandey, V. N. Shinde, R. L. Deopurkar, S. P. Kale, S. A. Patil and D. Pant, *Appl. Energy*, 2016, **168**, 706–723.
- 6 D. R. Lovley and K. P. Nevin, *Curr. Opin. Biotechnol.*, 2011, **22**, 441–448.
- 7 M. A. Rosenbaum and A. E. Franks, *Appl. Microbiol. Biotechnol.*, 2014, **98**, 509–518.
- 8 J. Wei, P. Liang and X. Huang, *Bioresour. Technol.*, 2011, **102**, 9335–9344.
- 9 X. Xie, M. Ye, L. Hu, N. Liu, J. R. McDonough, W. Chen, H. N. Alshareef, C. S. Criddle and Y. Cui, *Energy Environ. Sci.*, 2012, **5**, 5265–5270.
- 10 V. Flexer, J. Chen, B. C. Donose, P. Sherrell, G. G. Wallace and J. Keller, *Energy Environ. Sci.*, 2013, **6**, 1291–1298.
- 11 L. Jourdin, S. Freguia, B. C. Donose, J. Chen, G. G. Wallace, J. Keller and V. Flexer, *J. Mater. Chem. A*, 2014, **2**, 13093–13102.
- 12 B. Delord, W. Neri, K. Bertaux, A. Derre, I. Ly, N. Mano and P. Poulin, *Bioresour. Technol.*, 2017, **243**, 1227–1231.
- 13 G. Orive, E. Santos, D. Poncelet, R. M. Hernández, J. Pedraz, L. U. Wahlberg, P. De Vos and D. Emerich, *Trends Pharmacol. Sci.*, 2015, **36**, 537–546.
- 14 J. K. Park and H. N. Chang, *Biotechnol. Adv.*, 2000, **18**, 303–319.
- 15 H. Uludag, P. De Vos and P. A. Tresco, *Adv. Drug Delivery Rev.*, 2000, **42**, 29–64.
- 16 L. Rolland, E. Santanach-Carreras, T. Delmas, J. Bibette and N. Bremond, *Soft Matter*, 2014, **10**, 9668–9674.
- 17 N. Bremond, E. Santanach-Carreras, L. Y. Chu and J. Bibette, *Soft Matter*, 2010, **6**, 2484–2488.
- 18 K. Alessandri, B. R. Sarangi, V. V. Gurchenkov, B. Sinha, T. R. Kiessling, L. Fetler, F. Rico, S. Scheuring, C. Lamaze, A. Simon, S. Geraldo, D. Vignjevic, H. Domejean, L. Rolland, A. Funfak, J. Bibette, N. Bremond and P. Nassoy, *Proc. Natl. Acad. Sci. U. S. A.*, 2013, **110**, 14843–14848.
- 19 H. Domejean, M. de la Motte Saint Pierre, A. Funfak, N. Atrux-Tallau, K. Alessandri, P. Nassoy, J. Bibette and N. Bremond, *Lab Chip*, 2017, **17**, 110–119.
- 20 H. Yi, K. P. Nevin, B.-C. Kim, A. E. Franks, A. Klimes, L. M. Tender and D. R. Lovley, *Biosens. Bioelectron.*, 2009, **24**, 3498–3503.
- 21 H. Hou, L. Li, Y. Cho, P. de Figueiredo and A. Han, *PLoS One*, 2009, **4**, e6570.
- 22 A. Guiseppi-Elie, *Biomaterials*, 2010, **31**, 2701–2716.
- 23 A. K. Gaharwar, N. A. Peppas and A. Khademhosseini, *Biotechnol. Bioeng.*, 2014, **111**, 441–453.
- 24 A. A. Adewunmi, S. Ismail and A. S. Sultan, *J. Inorg. Organomet. Polym. Mater.*, 2016, **26**, 717–737.
- 25 I. Balberg, N. Binenbaum and N. Wagner, *Phys. Rev. Lett.*, 1984, **52**, 1465–1468.
- 26 D. R. Lovley, T. Ueki, T. Zhang, N. S. Malvankar, P. M. Shrestha, K. A. Flanagan, M. Aklujkar, J. E. Butler, L. Giloteaux, A.-E. Rotaru, D. E. Holmes, A. E. Franks, R. Orellana, C. Risso, K. P. Nevin and R. K. Poole, *Geobacter: The Microbe Electric's Physiology, Ecology, and Practical Applications*, Academic Press, 2011, vol. 59, pp. 1–100.
- 27 S. Banerjee, T. Hemraj-Benny and S. S. Wong, *Adv. Mater.*, 2005, **17**, 17–29.
- 28 M. J. O'Connell, P. Boul, L. M. Ericson, C. Huffman, Y. Wang, E. Haroz, C. Kuper, J. Tour, K. D. Ausman and R. E. Smalley, *Chem. Phys. Lett.*, 2001, **342**, 265–271.

- 29 J. Liu, A. G. Rinzler, H. Dai, J. H. Hafner, R. K. Bradley, P. J. Boul, A. Lu, T. Iverson, K. Shelimov, C. B. Huffman, F. Rodriguez-Macias, Y.-S. Shon, T. R. Lee, D. T. Colbert and R. E. Smalley, *Science*, 1998, **280**, 1253.
- 30 M. S. Strano, V. C. Moore, M. K. Miller, M. J. Allen, E. H. Haroz, C. Kittrell, R. H. Hauge and R. E. Smalley, *J. Nanosci. Nanotechnol.*, 2003, **3**, 81–86.
- 31 J.-M. Noel, L. Mottet, N. Bremond, P. Poulin, C. Combellas, J. Bibette and F. Kanoufi, *Chem. Sci.*, 2015, **6**, 3900–3905.
- 32 C. Mercader, V. Denis-Lutard, S. Jestin, M. Maugey, A. Derré, C. Zakri and P. Poulin, *J. Appl. Polym. Sci.*, 2012, **125**, E191–E196.
- 33 E. Secchi, T. Roversi, S. Buzzaccaro, L. Piazza and R. Piazza, *Soft Matter*, 2013, **9**, 3931–3944.
- 34 B. Vigolo, A. Penicaud, C. Coulon, C. Sauder, R. Pailler, C. Journet, P. Bernier and P. Poulin, *Science*, 2000, **290**, 1331–1334.
- 35 W. Bauhofer and J. Z. Kovacs, *Compos. Sci. Technol.*, 2009, **69**, 1486–1498.
- 36 S. Barrau, P. Demont, A. Peigney, C. Laurent and C. Lacabanne, *Macromolecules*, 2003, **36**, 5187–5194.
- 37 W. Lin, M. V. Coppi and D. Lovley, *Appl. Environ. Microbiol.*, 2004, **70**, 2525–2528.
- 38 D. R. Bond and D. R. Lovley, *Appl. Environ. Microbiol.*, 2003, **69**, 1548–1555.
- 39 G. Reguera, K. P. Nevin, J. S. Nicoll, S. F. Covalla, T. L. Woodard and D. R. Lovley, *Appl. Environ. Microbiol.*, 2006, **72**, 7345–7348.
- 40 K. P. Nevin, H. Richter, S. F. Covalla, J. P. Johnson, T. L. Woodard, A. L. Orloff, H. Jia, M. Zhang and D. R. Lovley, *Environ. Microbiol.*, 2008, **10**, 2505–2514.
- 41 K. B. Gregory, D. R. Bond and D. R. Lovley, *Environ. Microbiol.*, 2004, **6**, 596–604.
- 42 C. Dumas, R. Basseguy and A. Bergel, *Electrochim. Acta*, 2008, **53**, 2494–2500.
- 43 B. Erable, D. Féron and A. Bergel, *ChemSusChem*, 2012, **5**, 975–987.
- 44 J. P. Torella, C. J. Gagliardi, J. S. Chen, D. K. Bediako, B. Colón, J. C. Way, P. A. Silver and D. G. Nocera, *Proc. Natl. Acad. Sci. U. S. A.*, 2015, **112**, 2337–2342.